Utrecht University

Spontaneous creation of solitons by shock cooling sodium Bose-Einstein condensates

Author:
M.A. van Gogh
(3788180)

Supervisors:
prof. dr. P. van der Straten
P. Bons, MsC

June 18, 2014

Abstract

We study the formation of defects in a Bose-Einstein condensate as is described by the Kibble-Zurek mechanism. The mechanism describes the formation of defects when a second order phase transition is crossed at a finite rate. This is done by shock cooling or quenching the last part of the evaporative cooling process where the transition into the condensed state is made. This allows for the study of the amount of solitons formed as a function of the quench time with the ultimate goal of determining the critical exponents of the phase transition. The amount of solitons is predicted by the Kibble-Zurek mechanism to scale as the quench time to the power $-\alpha$, which we attempted to measure. The dynamics of solitons are also studied in order to determine the time scale on which they decay. This turns out to be in the order of 0.29 seconds, and thus an important factor, since we consider quench times in the order of seconds. When correcting for the decay on this timescale, it turns out that α is extremely sensitive to variations in the decay time and therefore we were not able to give conclusive evidence on a value for the exponent. Instead we estimate the value of α to be between 0.5 and 2, based on our measurements.

Contents

1 Introduction

Besides the well know states of matter encountered in day to day life, such as the solid, liquid and gaseous state, there exist a variety of exotic states that require more extreme conditions to form. One such state was theorized by Albert Einstein in 1924. After receiving a paper from the Indian physicist Satyendra Nath Bose on the quantum statistics of photons and translating it from English to German to have it published, he extended the idea to atoms. One of the predictions that came from that was that even at finite temperature, as long as it was sufficiently close to the absolute zero, which in this case means in the order of serveral hundred nanokelvins, macroscopic occupation of the energetic ground state would occur for a gas of bosons. This is what we now call a Bose-Einstein condensate (BEC).

Because it is such a complicated process to cool down a cloud of atoms to ultra low temperatures, it took over 70 years, until 1995, to finally show experimentally that this state of matter truly does exist. In 1995, Eric Cornell and Carl Wiemann at the Boulder NIST-JILA lab at the University of Colorado eventually succeeded in producing the first gaseous BEC by cooling a gas of rubidium-87 atoms to 170 nanokelvin. About four months later, Wolgang Ketterle and his group at MIT managed to create a BEC from sodium-23 atoms. For this, Eric Cornell, Carl Wiemann and Wolfgang Ketterle received the 2001 Nobel Prize in Physics.

In this thesis we will take a look at a theory concerning the consequences of speeding up the evaporative cooling stage in which the BEC is formed, known as the Kibble-Zurek mechanism (KZM). The prediction is that defects in the form of solitary waves, solitons, will form when the evaporative cooling is done more rapidly than is done normally. The goal of this thesis is to determine the scaling power of the amount of solitons as a function of the quench time, the time it takes for the cooling part in which condensation is achieved. This scaling in turn is linked to the critical exponents of the phase transition, which then determine the universality class of the phase transition.

We start by treating the theory of the condensate and the theory behind the Kibble-Zurek mechanism and solitons. Then an overview of the experimental setup will be given before showing how the data has been processed and presenting the results. We end by discussing factors that could have influenced the measurements and giving some possible future projects on this topic.

A brief summary of my research in layman's terms is given in Appendix A.

2 Theory

This research heavily relies on theory. In order to understand the research, the theory needs to be treated first. To start, the theory behind Bose-Einstein condensates is discussed. The general physics behind the BEC is treated and afterwards the Gross-Pitaevskii equation is derived and from that the Thomas-Fermi approximation is derived. Finally, the theoretical core of this thesis, namely solitons and the Kibble-Zurek mechanism, is treated which concludes this chapter.

2.1 Bose-Einstein Condensates

Bosons are particles with integer spin. One of their properties is that their wave function is symmetric under exchange of identical particles, from which follows that bosons are unaffected by the Pauli symmetrization principle and can occupy the same single-particle state. When a dilute gas of bosons is cooled below the critical temperature, condensation is achieved. One way to estimate the transition temperature is to consider the thermal de Broglie wavelength. The thermal de Broglie wavelength is given by:

$$\Lambda_{dB} = \sqrt{\frac{2\pi\hbar^2}{mk_BT}} \tag{1}$$

Here $\hbar$ is the Planck's constant divided by 2π, m is the mass of the atom, k_B is the Boltzmann constant and T is the temperature. One can see that the thermal wavelength scales with $\frac{1}{\sqrt{T}}$, so it follows that the wavelength increases as the temperature decreases, signifying that the lower the temperature, the more we observe the atoms like waves instead of particles. So at high temperatures the wavelength is negligible and the gas behaves classically. As the temperature is lowered, eventually the wavelength will become comparable to the mean interparticle spacing, which is in the order of $n^{-1/3}$, with n being the particle density. In this regime the thermal wavelengths will start to overlap and a BEC will be formed.

So an approximation is given by equating the mean interparticle spacing with the thermal wavelength and solving for the temperature:

$$T_c = \frac{2\pi\hbar^2 n^{\frac{2}{3}}}{k_B m}. \tag{2}$$

With the plausible value for the density of 10^{13} cm^{-3} and using the mass for sodium-23 atoms, we obtain a critical temperature of around 600 nanokelvin, which is certainly in the right order of magnitude.

Below the critical temperature, not all atoms instantly fall into the ground state. To quantify the fraction of atoms that are in the ground state as a function of the temperature, the condensate fraction is defined. The condensate fraction is given by:

$$\frac{N_0}{N} = 1 - \left(\frac{T}{T_c}\right)^3, \tag{3}$$

with N_0 being the amount of particles in the condensate and N the total amount of particles in the trap. Since negative values are not physical, the fraction is zero for temperatures larger than the critical temperature, which makes sense because only below the critical temperature a BEC can be formed.

The process of creating a BEC in our experiment will be discussed in Section 3.1.

2.2 The Gross-Pitaevskii Equation

In this section we will consider a model for the BEC which takes interactions into account and describes the properties of a zero temperature non-uniform Bose gas where the scattering length is much smaller than the mean interparticle spacing, the Gross-Pitaevskii Equation (GPE).

We shall derive the GPE as is done in Ref. [1].

In order to determine the energy of the many-body states we assume the Hartree approximation in which the wave function of the many-body state is equal to the product of the single-particle wave functions. Since we assume a temperature of absolute zero, we find that all particles in the cloud are in the ground state. So we find that the wave function of the N-particle system is given by

$$\Psi(\mathbf{r}_1, \mathbf{r}_2, \ldots, \mathbf{r}_N) = \prod_{i=1}^{N} \phi(\mathbf{r}_i), \tag{4}$$

in which all the single-particle wave functions $\phi(\mathbf{r}_i)$ are normalized. We also assume a mean-field approximation in which the long range interactions are neglected and we are left with an effective interaction in the Hamiltonian given by $U_{ij} = U_0\delta(\mathbf{r}_i - \mathbf{r}_j)$, where $U_0 = \frac{4\pi\hbar^2 a}{m}$, $\hbar$ is Planck's constant divided by 2π, m is the atom mass and a is the scattering length. The effective Hamiltonian is given by

$$H = \sum_{i=1}^{N} \left[\frac{\mathbf{p}_i^2}{2m} + V(\mathbf{r}_i) \right] + U_0 \sum_{i<j} \delta(\mathbf{r}_i - \mathbf{r}_j), \tag{5}$$

where $\mathbf{p}_i$ is the momentum operator and $V(\mathbf{r}_i)$ is the external potential. The energy of the state in eqn. 4 is found to be given by

$$E = N \int \left[\frac{\hbar^2}{2m} |\nabla\phi(\mathbf{r})|^2 + V(\mathbf{r})|\phi(\mathbf{r})|^2 + \frac{(N+1)}{2} U_0 |\phi(\mathbf{r})|^4 \right]. \tag{6}$$

Using the approximation that all single-particle wave functions are equal we introduce the wave function of the condensed state, given by $\psi(\mathbf{r}) = \sqrt{N}\phi(\mathbf{r})$ and with $n(\mathbf{r}) = |\psi(\mathbf{r})|^2$ the particle density. We can determine the energy in terms of the wavefunction, which gives us

$$E(\psi) = \int \left[\frac{\hbar^2}{2m} |\nabla\psi(\mathbf{r})|^2 + V(\mathbf{r})|\psi(\mathbf{r})|^2 + \frac{1}{2} U_0 |\psi(\mathbf{r})|^4 \right], \tag{7}$$

assuming that N is large. We want to minize this energy using the constraint that $\int \mathrm{d}\mathbf{r} n(\mathbf{r}) = N$, where N remains a constant. This is achieved by use of the method of Lagrange multipliers and we write $\delta E - \mu\delta N = 0$, where μ is the chemical potential. Using these constraints to minimize the energy gives us the time-independent Gross-Pitaevskii equation,

$$-\frac{\hbar^2}{2m}\nabla^2\psi(\mathbf{r}) + V(\mathbf{r})\psi(\mathbf{r}) + U_0|\psi(\mathbf{r})|^2\psi(\mathbf{r}) = \mu\psi(\mathbf{r}). \tag{8}$$

We will now focus on a harmonic potential wherein the trapping frequencies in two directions are identical. So for the external potential we can write $V(\mathbf{r}) = \frac{m}{2}(\omega_{rad}(x^2+y^2) + \omega_{ax}z^2) = \frac{m}{2}(\omega_{rad}(\rho^2) + \omega_{ax}z^2)$.

2.3 The Thomas-Fermi Approximation

When a large cloud of atoms is present, a good approximation of the condensate wavefunction can be made by solving the Gross-Pitaevskii equation after neglecting the kinetic term, $-\frac{\hbar^2}{2m}\nabla^2\psi(\mathbf{r})$, because it is small relative to the other terms. This leaves the equation

$$[V(\mathbf{r}) + U_0|\psi(\mathbf{r})|^2]\psi(\mathbf{r}) = \mu\psi(\mathbf{r}). \tag{9}$$

This equation can then be solved for $|\psi(\mathbf{r})|^2 = n(\mathbf{r})$ and a solution is given by

$$|\psi(\mathbf{r})|^2 = \frac{\mu - V(\mathbf{r})}{U_0}. \tag{10}$$

So in this approximation a condensate is found to be able to exist when the chemical potential μ is larger than the potential $V(\mathbf{r})$ and that its density is given by

$$n(\mathbf{r}) = \frac{\mu - V(\mathbf{r})}{U_0} = \begin{cases} \frac{1}{2}\frac{2\mu - m[\omega_{rad}(\rho^2)+\omega_{ax}z^2]}{U_0} & \mu > V(\mathbf{r}) \\ 0 & otherwise \end{cases} \tag{11}$$

and the size of the cloud in the axial and radial directions are given by $R_{rad} = \sqrt{\frac{2\mu}{m(\omega_{rad})^2}}$ and $R_{ax} = \sqrt{\frac{2\mu}{m(\omega_{ax})^2}}$.

With this approximation a model for the shape of the condensate has been obtained, which shall be used later on in a fitting procedure that is part of the data analysis process.

2.4 Solitons and the Kibble-Zurek mechanism

In this section the formation of defects in the form of solitary waves, or solitons, will be discussed. The necessary physics of the phase transition into the condensed state will be discussed to provide the background needed. Solitons will be discussed as both a mathematical solution of the time-dependent Gross-Pitaevskii equation and as an artefact of the second-order phase transition as predicted by the Kibble-Zurek mechanism.

2.4.1 Phase transitions

In order to understand the theory behind the formation of solitons, the relevant properties of phase transitions, specifically second-order transitions, need to be discussed.

We differentiate between two forms of phase transitions, namely the first-order transitions, where latent heat is involved, and the second-order, or continuous transitions. We shall focus on the second-order transitions, because the transition into the condensed state is of that type and has the properties related to the formation of defects.

The first of these properties is the existence of critical exponents. These describe the behaviour of certain physical parameters near the critical point at which the phase transition occurs. They are defined as

$$k = \lim_{T_R \to 0} \frac{\log |f(T_R)|}{\log |T_R|}, \tag{12}$$

where T_R is the relative temperature defined as

$$T_R = \frac{T - T_C}{T_C}. \tag{13}$$

In BEC's two such quantities are the correlation length, also known as the healing length, and the relaxation time, which we shall describe in more detail later on. While it has not been proven as of yet as far as I know, it is generally accepted that these critical exponents are universal, which means that they do not depend on the details of the system, but only on the dimension of the system, the range of the interaction and the spin dimension.

Closely related to critical exponents is the concept of universality classes. All phase transitions in a certain system belong to a universality class and for systems that belong to the same universality class, the critical exponents will be identical. In this way, one can know the behaviour of a very complex system near the critical point through measuring the critical exponents of a simpler, or at least more easily measurable, system that belongs to the same universality class. This is of course assuming that one can find such a simpler system and know that it belongs to the same universality class.

Another concept that has to be introduced is the order parameter, which is a measure of order in a system. This order parameter is usually zero when above the critical point and larger than zero below it. In a BEC, the role of order parameter is fulfilled by the condensate wavefunction, which is defined up to a constant phase. This phase factor is crucial in the formation of solitons as will be shown in Section **??**.

2.4.2 Mathematical solitons

The Gross-Pitaevskii equation as derived in Section 2.2 is useful to describe the equilibrium structure of the condensate. Solitons, however, arise due to the dynamics of the condensate, so in this section we will concern ourselves with the time-dependent version of the Gross-Pitaevskii equation and is used to describe the condensate dynamics.

The time-dependent Gross-Pitaevskii equation is given by

$$\imath\hbar\frac{\partial\Psi(\vec{r},t)}{\partial t} = [-\frac{\hbar^2}{2m}\nabla^2 + V(\vec{r}) + \frac{4\pi\hbar^2 a_s}{m}|\Psi(\vec{r},t)|^2]\Psi(\vec{r},t). \tag{14}$$

Since interaction terms can no longer be ignored in this equation, one would expect it to be difficult to find analytical solutions to this equations. It turns out that there actually are analytic solutions to this equation in the regime where interaction terms are important. These solutions are in the form of solitons, or solitary waves, that can propagate through the condensate without changing form.

These solutions exist due to non-linearity and dispersion in the Gross-Pitaevskii equation and the solitons preserve their form because these two effects nullify each other. In this case the non-linear term comes from the interaction between particles and the dispersion is given by the Bogoliubov dispersion, given by

$$\omega^2 = \frac{nU_0}{m}q^2 + \frac{\hbar^2 q^4}{4m^2}, \tag{15}$$

where n is the equilibrium density, ω is the frequency and q is the norm of the wave vector. This relation arises from the hydrodynamic equations derived from the time-dependent Gross-Pitaevskii equation , which will not be discussed in this thesis. The mathematical details on this can be found in Ref. [1].

A very important remark about solitons is that they are a purely one-dimensional solution, while the condensates are in principal three-dimensional, which has consequences later on when the lifetime of solitons is treated.

2.4.3 Formation of solitons in a BEC

In order to discuss the formation of solitons in the BEC, more concepts as well as the Kibble-Zurek mechanism (KZM) need to be introduced. The Kibble-Zurek mechanism (KZM) is a theory that describes the non-equilibrium dynamics of a second-order phase transition that is traversed at a finite rate. In this scenario, critical slowing down and spontaneous symmetry breaking occur. It was originally intended to study the effects of rapid phase transitions in cosmology and was later extended to all continuous phase transitions, both classical and quantum phase transitions, that are traversed at a finite rate [2]. The KZM predicts the formation of defects in systems where continuous phase transitions are crossed at a finite rate and the density of the defects scales with the critical exponent of the phase transition.

To understand the process, the concepts of critical slowing down and spontaneous symmetry breaking will need to be explained. A didactic example shall be used to contribute to the intuitive understanding of this concept.

Spontaneous symmetry breaking in a physical system means that the underlying laws of the system, possibly equations of motion or a Lagrangian, is still invariant under a symmetry transformation, but the system as a whole is not. An often used example is the ball on a "mexican hat" potential. It has an unstable state in the center where it is symmetric under rotation of the system. Eventually even the tiniest perturbation will make the ball roll down into

the true minimum of the potential where it will take a random position on the ring of minima, corresponding to a certain phase on the ring. The system is now no longer invariant under rotation and the symmetry has been spontaneously broken. In a BEC transition a similar event happens. When the critical temperature has been reached, which happens first in the center of the trap, symmetry is spontaneously broken when the phase of the order parameter is fixed at random. This is a very important concept for the formation of solitons.

Critical slowing down is the divergence of the equilibrium correlation length ξ and the relaxation time τ at the critical temperature. The correlation length, also known as the healing length and coherence length, is the length at which the wavefunction tends to its bulk value after being subjected to a local perturbation. It is defined such that the kinetic energy term and interaction term of the time-independent Gross-Pitaevskii equation are equal when varied on a scale of ξ. Note that this is a static property. The relaxation time is the time scale on which a perturbed system will return to its equilibrium. Note that this is a dynamic property.

The KZM also predicts the behaviour of these two quantities near the critical point and is given by

$$\tau(t) = \frac{\tau_0}{|T_R(t)|^{\nu z}} \tag{16}$$

and

$$\xi(t) = \frac{\xi_0}{|T_R(t)|^{\nu}} \tag{17}$$

for the relaxation time and the healing length respectively, where τ_0 and ξ_0 are constants [5]. Since the relative temperature goes to zero at the critical temperature, the relaxation time and the healing length will diverge at this point. The exponents ν and z are respectively the static critical exponent and the dynamic critical exponent of the phase transition. The main goal of this research is to attempt to determine their values and the universality class of the phase transition.

When the phase of the order parameter is chosen through SSB, information about that phase can travel. When the system is cooled sufficiently slowly, the information of the phase can keep up with the speed at which the temperature can drop below the critical temperature further away from the trap center. This means that all condensates that nucleate will pick the same phase as the condensate in the center of the trap. The phase information can not travel faster than the corresponding characteristic velocity given by

$$s(t) = \frac{\xi(t)}{\tau(t)} = \frac{\xi_0}{\tau_0}|T_R(t)|^{(z-1)\nu}. \tag{18}$$

The information propagates through spin waves, also known as second sound.

However, when the system is cooled down more rapidly, known as quenching or shock cooling, the temperature can drop below the critical temperature through most of the trap before information regarding the phase of the order parameter can travel to those outer regions. In these regions, condensates can form, because the temperature is below the critical temperature, and because no information regarding the phase of other condensates has had time to reach that area yet, a phase will be selected at random through SSB. Multiple condensates

can be formed in the trap, all with their own different phases. These condensates will grow and eventually meet, but they cannot merge because they have incompatible phases. At the border of two of such regions a soliton is formed to bridge the gap in phases and can be regarded as a continuous phase slip. This manifests itself as a density depletion of the condensate, which lies along the radial axis of symmetry. This is due to the difference in timescale between the dynamics along the radial and axial axes. Because of the much tighter confinement in the radial direction, the timescales are much shorter and, as shall be discussed in Section 2.4.4, solitons are transversely unstable and will be destroyed swiftly when not positioned along the radial axis.

The KZM predicts that the number of solitons scales as:

$$d \propto (\frac{\tau_0}{\tau_Q})^{\frac{1+2\nu}{1+\nu z}} \equiv (\frac{\tau_0}{\tau_Q})^{\alpha}, \tag{19}$$

where d is the amount of solitons and τ_Q is the quench time, the time it takes to cool the system through the critical temperature [5]. How this is defined in our experiment will be discussed in the next section on our experimental setup.

The solitons that are formed have a width in the order of the healing length, which is given by

$$\xi_0 = \frac{1}{\sqrt{n_0 4\pi a}}, \tag{20}$$

where n_0 is the density of the condensate assuming uniformity and a is the scattering length, which is calculated as given in Ref. [3]. Using the realistic values for our experiment of $n_0 = 10^{19}$ and $a = 60 * 10^{-9}$ places the healing length at below a micron.

Solitons in which there is a density depletion are called dark solitons. Dark solitons themselves are divided in two subclasses, namely gray and black solitons. Black solitons are formed when the phase difference is exacly π, which corresponds to a full depletion of the condensate, meaning that the density in the center of the black soliton is zero. Gray solitons are formed when the phase difference is less than π and does not fully deplete the condensate. Black solitons are fully stationary, while gray solitons will oscillate through the condensate. In our setup, since the phases are fully random, black solitons are non-existant, so the only solitons we observe are gray ones. Besides dark solitons there also exists bright solitons, which correspond to density increases. Dark solitons are stable for condensates with attractive interaction, such as ours, while being unstable for condensates with repulsive interaction. Bright solitons are the other way around and are unstable for our system and as such are not observed.

The way we experimentally create solitons in a BEC will be discussed in Section 3.1.1.

2.4.4 Soliton decay

The solitons that were studied do not carry a topological charge [4], so they are not topologically protected, and as such can decay and cease to exist without having to reach the edge of the condensate first. This turns out to be an important factor in determining the critical exponents of the phase transition

and the decay rate will be experimentally determined in order to correct for this mechanism in the section on results.

As described before, solitons are a phase slip between two condensate sections that carry different phase and as such are seen as a density depletion of the condensate. One can assign an energy to the soliton, determined by condensate density and the depth of the soliton. When the soliton loses this energy through the mechanisms which shall be described next, the soliton gradually starts to lose depth and eventually the phase slip will be nullified, which marks the end of the soliton.

There are three main mechanisms that contribute to the decay of solitons ([7],[8]).

The first is interaction with the thermal cloud. From the formula of the condensate fraction, one can deduce that for any condensate where the temperature is larger than zero, which will be the case for any realistic experiment, there will still a fraction of the atoms not in the ground state and form a thermal cloud. The soliton can interact with the cloud and lose energy to it. The lower the temperature, of course, the more this mechanism will be suppressed. Note that due to interactions between particles, there will still be a thermal cloud when the temperature does reach zero, but its effect will be negligible.

The second is through the emission of phonons, or sound waves. When solitons do not carry a full π phase slip, they will not be stationary and will oscillate through the condensate. The solitons have a velocity dependent on the phase slip they carry. For a phase slip of π, their velocity will be zero and the density depletion is maximal, while for a phase slip of zero, their velocity will be equal to their maximal velocity given by the speed of sound and the density depletion will be zero, making them indistinguishable from the background. When solitons move, they will either move up or down the potential slope and with that either accelerate or decelerate. Like particles, they radiate energy when accelerating or decelerating, where this is done in the form of sound waves. When solitons lose energy, they start to oscillate faster, a process known as anti-damping, leading to a quick decay of the soliton. However, in the case of harmonic potentials, it has been found that the solitons can reabsorb the emitted phonons, stabilising them against this type of decay. When anharmonicities in this potential are present, this equilibrium may once again be destroyed [9].

A third possibility stems from the fact that a soliton is purely 1-dimensional while the condensate is 3-dimensional. This gives rise to the so-called snake-instability, or transverse instability, in which the soliton breaks up into vortex-rings that disappear. For condensates that have a high aspect ratio, this mechanism is expected to be suppressed.

3 Experiment

To achieve the creation a BEC, a complex setup involving lasers and magnetic fields is needed. The setup as it stands in our experiment will be explained and the process of laser cooling will be discussed. To determine the critical exponents of the phase transition, solitons need to be created. The method used in this research will be shown. Imaging is done in order to do measurements on the condensates and solitons. Two methods of imaging are currently in use in our experiment, namely absorption imaging and phase contract imaging. Both will be discussed briefly.

3.1 Experimental Setup

In our experiment we use sodium-23 atoms to create a BEC. To accomplish this, a complex setup is needed to sufficiently cool down the atoms, utilising both laser cooling and evaporative cooling. Both types of cooling will be explained briefly.

First sodium is heated in the first oven chamber to about 600K, which corresponds to a speed of around 800 m/s. A small diaphragm is used to only have a tight beam of sodium atoms leave this chamber. In the second oven chamber another small diaphragm is used to further tighten the beam of sodium atoms. In this chamber there is also channel leading back from this chamber to the first one. This is to allow for recirculation of the sodium atoms into the first chamber in order to prevent the build-up of sodium in the second chamber. The third chamber hosts a diffusion pump to prevent build-up of atoms in that chamber.

After the oven, and focussed into a tight beam, the atoms enter the Zeeman slower. In this part laser cooling is used to cool down the atoms. Laser cooling is done as follows. A laser beam is shone in the opposite direction of where the atom is travelling. The atom can absorb a photon, which puts the atom into an excited state, slowing down the atom by an amount equal the the momentum of the absorbed photon. The atom will then decay back into the ground state, re-emitting a photon. The emission of this photon is spontaneous, in this case meaning that the direction it is emitted in is given by the dipole radiation pattern. Averaged over a large amount of emissions, the net velocity gain from the photon emission will be zero, therefore the atom will be slowed down.

In order for the atoms to absorb photons, the laser beam has to be resonant with a transition of the atom. The transition that is used for slowing down the atoms is the $3^2S_{1/2}, F_g = 2 \rightarrow 3^2P_{3/2}, F_e = 3$ transition, which from now on will be referred to as $F_g = 2 \rightarrow F_e = 3$. The hyperfine splitting of sodium is shown in Figure 1. The laser beam that is used for this purpose is known as the Zeeman beam. In this process a second beam, which is called the repump beam, is also necessary. This beam is required because the atoms can also make the transition $F_g = 2 \rightarrow F_e = 2$, which can then decay into the $F_g = 1$ state, which is a state that does not interact which the Zeeman beam. So this second beam is tuned to the $F_g = 1 \rightarrow F_e = 2$, which can then decay into the $F_g = 2$ state. This repump beam effectively drives the transition $F_g = 1 \rightarrow F_g = 2$. While the transition $F_g = 2 \rightarrow F_e = 2$ does not have a high chance to occur, the amount of photons needed to slow the atoms down is very large, so the repump beam is necessary

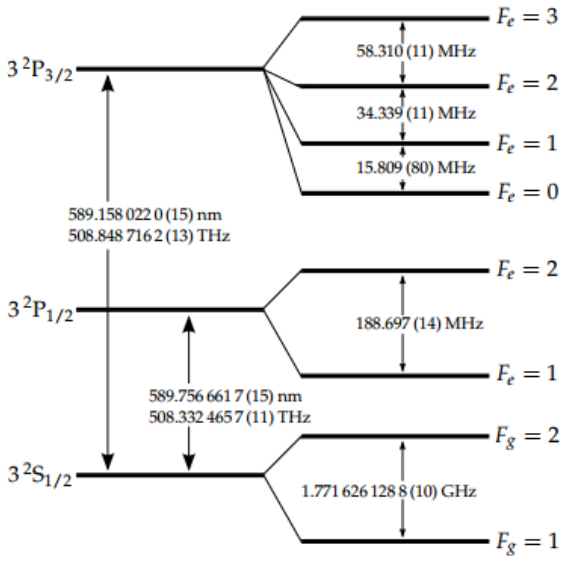

Figure 1: The hyperfine splitting of sodium with the wavelengths being those in vacuum. (Picture from Ref. [3])

to prevent significant losses. One of the complications of this technique is that when the atoms slow down, they stop being resonant with the laser due to the Doppler shift of the light in the atom frame of reference. To counter this, an inhomogeneous magnetic field, which is highest at the oven and lowest at the end of the Zeeman slower, is used, such that the Zeeman effect nullifies the effect of the Doppler shift, thereby keeping the atom resonant with the Zeeman beam throughout the Zeeman slower. The distinction between the slowing and cooling of atoms needs to be made here. The process above describes how the atoms are slowed individually, but it order to cool a system, not only does the mean velocity need to be lowered, the velocity distribution needs to be compressed. This also happens in the Zeeman slower, because atoms that have a higher than average velocity will remain resonant with the laser beam longer than the other atoms, while atoms with a below average energy will not be resonant with the beam until later in the slower due to the inhomogeneous magnetic field. So not only are the atoms slowed, the system is cooled as well.

After exiting the Zeeman slower, the atoms are caught in a trap. This is done using a dark spot magneto-optical trap, the MOT. In this trap, the atoms are trapped using both a magnetic field and laser beams. The magnetic field is a quadrupole field, generated by putting two coils in an anti-Helmholtz setup, generating a field gradient of 5 G/cm. Along with this field, six laser beams, which are slightly red-detuned with respect to the atomic transition, propagating along both directions of the three main axes are present. These beams are circularly polarized and if one beam on an axis is polarized one way, the counterpropagating beam will be polarized the other way. The lasers are detuned about 1.5 linewidths below the $F_g = 2 \rightarrow F_e = 3$ transition. With this setup, when an atom moves in one direction, from the atom frame of reference, the

beam coming from the direction the atom is moving is closer to the resonance frequency than the beam it is moving away from, therefore absorbing more photons from the beam it is moving towards, which results in a net force slowing the atom. This holds for any direction it tries to move in, so the laser beams will always stop the atom. Because of the collisions between the atoms in the trap, the atoms will display a random walk behaviour and slowly diffuse. It is clear that with the laser beams alone the particles cannot be trapped. Depending on the spin state of the atom, they are either more or less sensitive to one of the beams due to the circular polarization. When an atom crosses the zero of the magnetic field, which is the center of the MOT by definition, their spin state will be flipped and they will be more sensitive to the other beam than they were before the crossing. So we have two forces that act upon the atom, depending on velocity and position. The net result is that the atom will always be pushed back into the center of the trap.

However, this only holds for atoms in the $F_g = 2$ state, however, and atoms in the $F_g = 1$ state will be lost, because they do not interact with the light. So, just like in the Zeeman slower, a repump beam is necessary to drive the $F_g = 1 \rightarrow F_g = 2$ transition. In order to prevent unnecessary heating effects, the repump beam has a dark spot in its center such that only atoms that are not in the center of the trap can get repumped. This allows for atoms in the center of the trap to decay to the $F_g = 1$ state which reduces radiation pressure in the center of the trap significantly, allowing for much higher densities of cold atoms in the MOT.

When one wants to do an experiment, the atoms are transferred to the magnetic trap (MT), to facilitate evaporative cooling to further cool down the atoms to below the critical temperature. We use a harmonic trap that is rotationally symmetric around the z axis. In this trap there is a potential minimum in the center of the trap, where the effective field is zero. However, this trap can only contain atoms that are in the $|F = 1, m = -1>$ configuration. Atoms with $m = 0$ are not sensitive to magnetic fields and as such cannot be contained in purely magnetic traps and as such are lost when transferred to the MT. Atoms in the $m = \pm 1$ state are attracted towards high magnetic fields and low magnetic fields for $m = +1$ and $m = -1$ respectively and are suitably called high field seekers and low field seekers. Since creating a maximum of a magnetic field in space is forbidden by Maxwell's equations, the high field seekers are also lost and only the low field seekers are trapped in the minimum of the MT.

Once the atoms are transferred to the MT, we can start the process of evaporative cooling. We use a radio frequency (RF) antenna to create an RF-field that transitions atoms that have an energy at a certain threshold, determined by the RF-field, to the $|F = 1, m = 0, 1>$ states, thereby removing them from the trap. Since the particles that are removed have a higher than average energy, the average energy of the remaining atoms will be lowered by the removal of the particles, lowering the temperature of the cloud. This is known as spilling and is only a part of the process. A more effective part of the cooling stems from the collision between atoms. When two atoms in the trap collide, one will obtain a higher energy, while the other will lose energy. When this higher energy particle is then removed by means described above, not only is a higher than average particle removed from the trap, it cooled another atom in the process, making

this much more efficient than spilling alone. This threshold is lowered slowly to remove the highest-energy particles from the trap while allowing the cloud to stay close to thermal equilibrium. This cooling process is capable of bringing the temperature well below the critical temperature.

3.1.1 Creating solitons

The first step to studying solitons is to create them. In order to create solitons, we slightly modify the evaporative cooling process described above. As described by the Kibble-Zurek mechanism in Section 2.4.3, the second-order phase transition is crossed at a finite rate, which will cause defects to form, based on the swiftness of the crossing. So we want to modify the speed at which the critical temperature is crossed. We do this by selecting a region around T_c in which we drastically speed up the ramping down of the RF-field. This is accomplished by selecting a point a little above T_c and a point beneath T_c in which we let a second RF antenna, which is made resonant for the frequency around which the transition into the condensed state is made, lower the threshold linear in time, but more quickly than is done normally. This is known as the quench and the time it takes to cross the region is known as the quench time τ_Q. Doing this will allow us to meet the criteria for creating solitons as described in Section 2.4.3.

3.2 Imaging Techniques

In order to obtain information about the condensate, there are two methods that are frequently used within our group, namely absorption imaging and phase contrast imaging. Both will be discussed, but since all of my experiments are done using absorption imaging, I shall only discuss phase contrast imaging briefly because it is an interesting technique and could possibly be used in future research in solitons in an BEC.

Absorption imaging is done by sending a pulse of resonant laser light through the condensate, allowing us to obtain the optical density. When this light is sent through the condensate, a portion of the photons gets absorbed by atoms in the condensate. Using a CCD camera, one can determine the amount of photons that passed through the condensate without getting absorbed. Comparing this with the total amount of photons that were sent out, one can determine the optical density. More mathematical details can be found in Ref. [10].

When imaging with this technique, three images are created in rapid succession. The first is an image of the condensate, as desired, the second image is the same, but without the condensate to determine the background, and the third is an image without light, to determine the camera noise. One can then reconstruct the final image by subtracting the noise image from the condensate and background image and then dividing the modified condensate image by the modified background image:

$$I_{final} = \frac{I_{condensate} - I_{noise}}{I_{background} - I_{noise}}. \tag{21}$$

This gives us the transmission and the value of the pixels in the image will

be between 0 and 1. Since the three images are not taken at the same exact moment, there can still be fluctuations and as such the final image will not be entirely noise free and may still contain effects such as interference patterns. In the section on the post-processing of the images methods will be described to further reduce these effects.

Upsides to this technique are that it is a relatively simple way of imaging a BEC and one can remain below saturation in order to reduce noise in the images.

Downsides are that it is a destructive way of imaging, destroying the condensate in the process, and that for very high densities it can become impossible for the light to get through, meaning that the density cannot be derived from the image. This means that in situ measurements become difficult. Because it is a destructive method, it is also not the most suitable way of studying condensate dynamics.

To get around the problem of too high optical densities, we build in a time of flight (ToF). During this ToF, we turn off the trap allowing the condensate to fall and expand because it is no longer confined. This way the optical density will be reduced and the laser pulse can more easily penetrate the condensate. In our elongated condensates the radial confinement is stronger than the axial confinement, meaning it will expand faster in the radial direction during the ToF.

Phase Contrast Imaging, in contrast to absorption imaging, is a non-destructive way of imaging the condensate. In this technique a beam of near-resonant light is sent through the condensate. Considering the light as an electric field, part of the field has been diffracted after passing through the cloud and accumulated a complex phase, while the rest of the field remains unaffected. The amount of diffraction depends on the complex refractive index of the cloud, which itself depends on the complex polarizability of the atoms. The phase shift which is measured in PCI is proportional to the real part of the polarizability, while the imaginary part causes the scattering which is measured in absorption imaging. Because the polarizability is constant for a fixed detuning, the phase shift is directly related to the density. When detuning from resonance, the imaginary part get smaller much faster than the real part, allowing for measuring the phase shift while the absorption is small. The details on this method are given in chapter 3 of Ref. [3].

The upside to this technique is that it is a non-destructive method, allowing for making a sequence of images of the same condensate in situ. This means that it is more suitable for studying the dynamics of the condensate than AI. The reason it has not been used in my experiment is because of its resolution, which is 3 μm, which means that any feature smaller than 10 μm will not be clear. As shown in Section 2.4.3, the solitons that were studied are in the order of the healing length, which was smaller than a micron, which means that in situ they are less than the required 10 μm. Only after a ToF would they have expanded enough to be imaged, which in turn defeats the purpose of using PCI. Maybe in a future experiment a way can be found to circumvent this problem, because being able to track a soliton through its lifetime would provide valuable information on its (primary) decay mechanism amongst other properties.

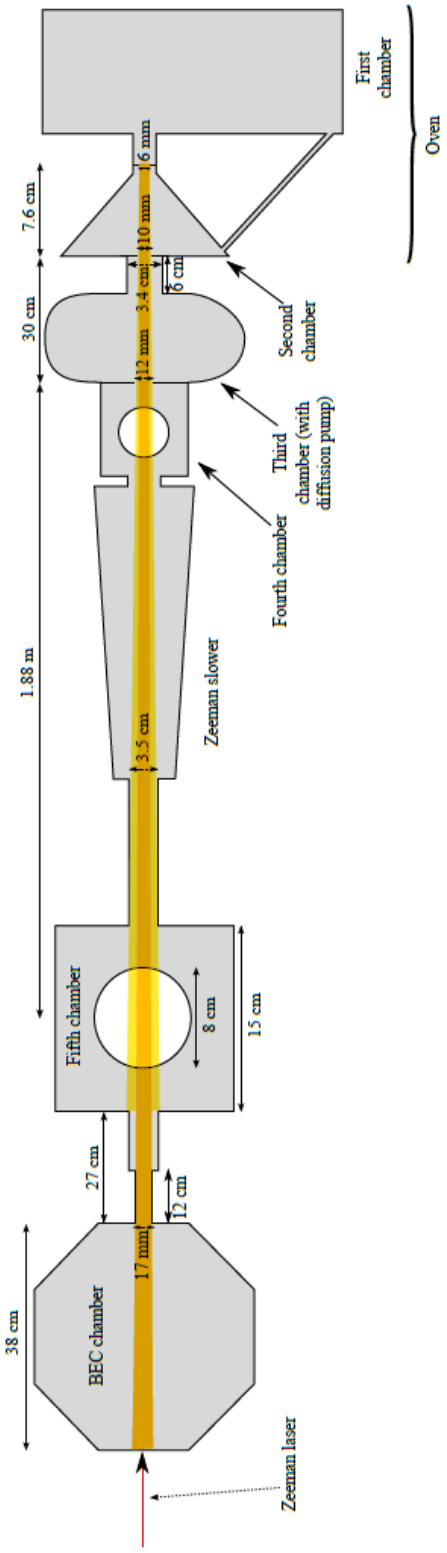

Figure 2: Schematic of the experimental setup. Image from Ref. [11].

4 Results

In this section the results will be presented. The routine of post-processing the images in order to reduce noise and other unwanted effects is treated. The code used to automatically count the number of solitons in the images will be explained. After that we move on to how the obtained data was processed and analysed while showing the obtained results. This includes measurements aimed at determining the critical exponents of the system and a measurement of the decay time of solitons.

4.1 Post-processing of images

In order to be able to automatically count the number of solitons in an image, you want the image to be as clean as possible. To accomplish this, two main techniques are used in my post-processing routine, being singular value decomposition (SVD) and fast Fourier transforms (FFT) together with applying masks.

The first of the two techniques to be applied is SVD. This technique is based heavily on linear algebra and utilises the pseudoinverse of the image to reconstruct the background. The technique discriminates between static and dynamic features, where it is able to pick out the dynamic features of the background, which is primarily noise, and discard them. Only the intuitive explanation shall be given here. For the curious reader, the mathematical details are given in Ref [10]. This technique uses multiple images to clean up one image in that series. All of the background images from the series are takes and a new background image is constructed by making a linear superposition of those backgrounds. This technique reduces the effect of noise in background shots because effects that only occur in a few of the background images will be reduced and mainly pieces that occur in most background, and as such are probably really part of the background instead of noise, will be left in the final image. This way a new background is found that contains less noise than the original background image, which translates into a less noisy final image.

Although this technique is commonly referred to as SVD, SVD is actually a mathematical technique that is used in the computation of the pseudoinverse of the image, which is then used in the reconstruction of the background. So this method is actually one of the many applications of SVD and not the actual technique itself. For simplicities sake it will still be referred to as SVD in the rest of this thesis.

After the initial cleanup using SVD, a further clean up is done using FFT and masks. By applying a FFT to the image data, we transfer it to the frequency domain. Especially periodic effects such as interference patterns become very clear and can easily be removed by setting the corresponding components of the matrix to zero. An example of how interference patterns can be removed through this technique is given in Figure 3. After transforming back, the original image is generally no longer recognisable, but the solitons are still visible. We then sum all the columns of the image to obtain a 1-dimensional spectrum. In this spectrum the solitons are manifested as peaks in the spectrum and by comparing spectra to their images we have experimentally determined a minimum height

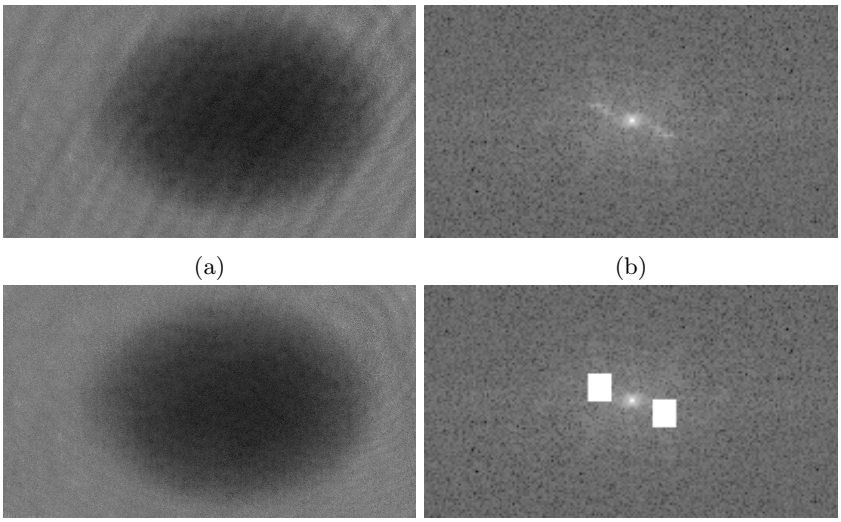

Figure 3: a: Image of the condensate before applying FFT and masks, b: Fourier transform of the image, c: Image of the condensate after applying FFT and masks, d: The mask applied to the Fourier transformed image

and a width region in which the solitons can be found. We then use these criteria in a program that for all peaks in the spectrum checks whether they satisfy the conditions. An example of this is given in Figure 4.

As an additional selection criterium we use the size of the condensate. As shown in Ref. [6], condensates with a lower amount of particles will produce more solitons on average given the same quench times. Therefore it is important to only compare condensates of roughly the same size. To quantify this, a 2D Thomas-Fermi profile, along with a 2D Gaussian profile is fitted to each image. The Gaussian is to determine the size of the thermal cloud, while the TF profile is to determine the profile of the actual condensate. From this the size of the condensate is extracted and can be used as an additional selection criterium before counting the solitons in it. Note that in the spectra as seen in Figure 4 this criterium is already applied and that the spectrum outside of the condensate range is set to 0.

4.2 Statistical analysis and methods

The Kibble-Zurek mechanism is a stochastic process. So when two measurements are done under the same circumstances, one won't necessarily find the same number of solitons both times. Now it is also clear that the amount of solitons one finds in any given measurement is an integer, so one expects that the amount of solitons found given the same parameters would have to be distributed according to a discrete distribution. Given the nature of the KZM, it is a logical step to consider the Poisson distribution as a prime candidate. I have not found anything in the theory suggesting that this has to be governed by Poisson statistics, but the empirical evidence obtained during the course of

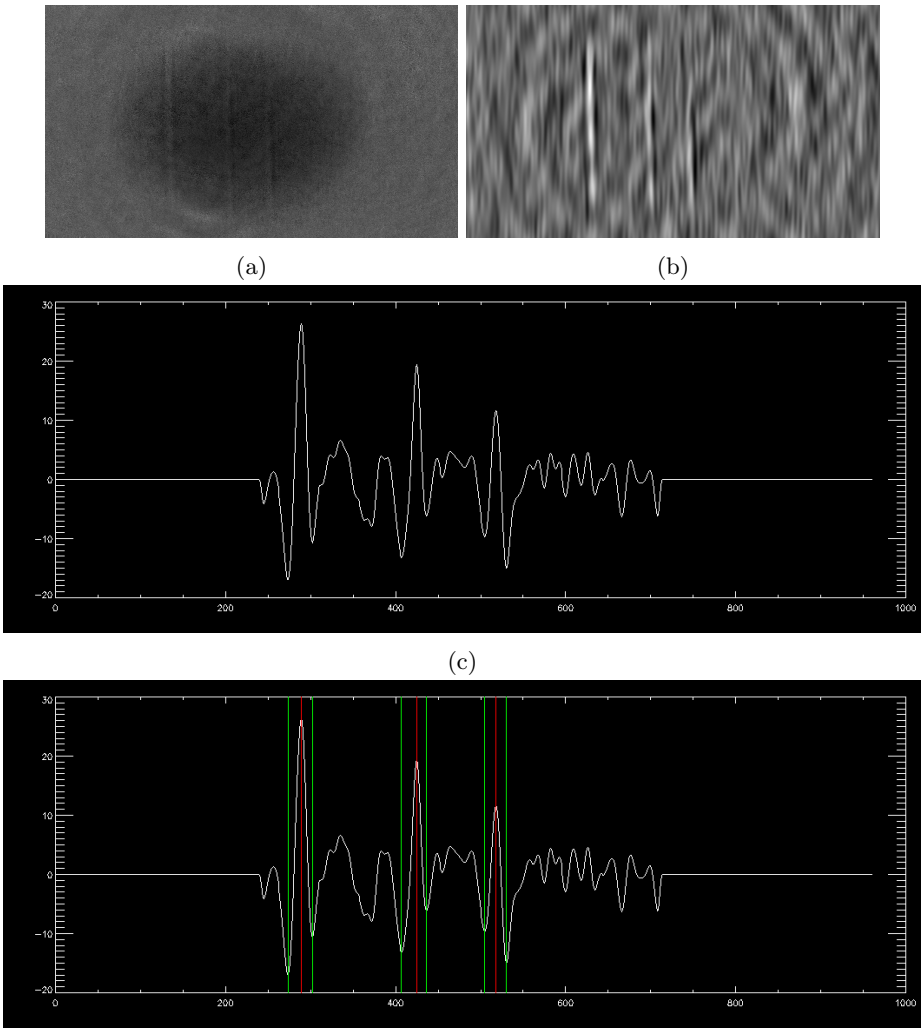

Figure 4: Overview of the routine performed on the measurements.
a: Image of the condensate before the routine, b: Image after the FFT routine, c: Spectrum after summing over all columns, d: Spectrum with the peaks as counted by the program.
The red line indicates the maxima of the soliton peaks, while the green lines signify the minima of the peaks

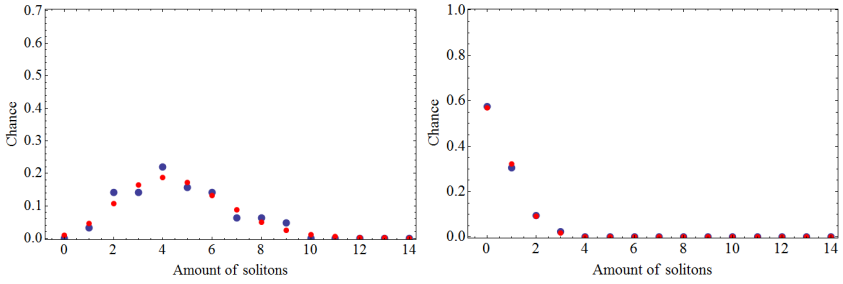

(a) (b)

Figure 5: Both images from the series on the decay time which will be presented in Section 4.3. The blue points are measured data while the red points are the points corresponding to the best Poisson fit.
a: Waiting time = 0.25 sec, sample size is 64.
b: Waiting time = 1 sec, sample size is 85.

this research does suggests that this is the case. Figure 5 makes a good case for this statement.

First the measurements on soliton decay will be given. This should give us a correction factor to use on the data obtained for the determination of the exponent. The way these measurements were done was by selecting a quench time and fixing that. In this case, the quench time was fixed at 2s. Then a holding time was introduced and afterwards the condensate was expanded and imaged in the usual way. So we have a fixed quench time and a variable holding time after the quench that allowed the solitons to move through the condensate and dissipate before the ToF, which in our experiments was set at 70 ms. Then the amount of solitons left were counted and plotted as a function of the holding time. This allowed us to define a half-life time for solitons. This is, of course, assuming exponential decay. Once again, I have not found anything in the theory suggesting that the decay of solitons is exponential, in fact, the decay is a continuous process when done through anti-damping and therefore most likely not exponential, but it seems to be a good approximation and easy to use in a correction factor, therefore we shall use the half-life time for pragmatic reasons.

After that the results of the measurements on the exponent will be given. The measurement were done in a similar way to the measurements done on the decay time, but now we do not make use of a holding time and the quench time is varied. The results on determining the influence of condensate density and aspect ratio will also be presented. These were done in the same way, but in order to achieve lower densities, the cooling process prior to the quench stage is done less efficiently and for lower aspect ratios the trap frequencies are varied.

The analysis is done is by taking the data and for each quench time or waiting time, a Poisson distribution was fitted to determine its mean value. The error in each point is given by the standard formula for calculating the standard deviation of the mean, $\frac{\sqrt{\sigma}}{\sqrt{N}}$, where N is the amount of samples for that given value of the quench time or wait time and σ in this case is the root of the mean amount of solitons. For the measurements on the decay time, the general model

for exponential decay, $c \cdot 2^{-\frac{t}{\tau_{1/2}}}$, is fitted to determine the half-live time $\tau_{1/2}$. For the measurements on the exponent, the curve $c \cdot \tau_Q^{-\alpha}$ is fitted in order to determine the exponent α. In both fits, the weights of each point are given by the usual formula, which is $1/error^2$. In this case the weight of each point is equal to the amount of samples for that given point.

4.3 Decay

Preliminary measurements were done and the results are shown in Figure 6. We used two different condensate sizes in order to investigate size dependence of the decay time. As is shown, the decay time does seem to vary with different sizes, but since the amount of measurements per data point is quite low, the results are not conclusive on the influence of size and the two values are within the error margins. The preliminary measurements find a decay time of a quarter and a third of a second for the bigger and smaller condensates respectively. This means that the decay time is a very relevant factor when considering the measurements trying to determine the exponent, since the quench times are in the order of seconds.

These measurements paved the way for a more extensive measurement with a significantly larger sample size per point. This was also done and the results are shown in Figure 7. The result of this series of measurements also gives us a half-life time of around 0.3 seconds and is in the same order of magnitude as the preliminary measurements.

To find out more about the way the solitons in our experiment decay, The heights of the peaks of the solitons were recorded during the analysis of the measurements. When solitons decay through means of anti-damping, one expects to see that the solitons gradually lose their contrast and with that, the peaks become shallower. The result of this is shown in Figure 8. Note that this is a very coarse determination. As peaks become shallower, they may drop below the threshold for the program to count it as a soliton, which may skew this data. The green points in Figure 8 are practically at the cut-off point, hence that the minima are almost the same for all waiting times. From the data we find that the mean depths do not significantly differ between the waiting times. The maximum values do seem to get somewhat lower with the waiting time, indicating the possibility that solitons lose their energy over time. Note that, assuming a decay through gradual loss of energy, the mean heights of the peaks do not necessarily get smaller. Due to the decay, the lowest energy solitons will die out first, while the higher energy solitons only lose a part of their energy. This may cause the mean to remain stable, while the maxima of the heights gradually gets smaller. However, from these measurements, we cannot really draw a definite conclusion, because the way of recording the heights is somewhat arbitrary and due to the extreme effects of the post-processing, I cannot be sure that peak height in the final spectrum has a one to one correspondence with the soliton depth. The best way to probe the primary decay mechanism would be to utilize non-destructive imaging, which would be a great future research.

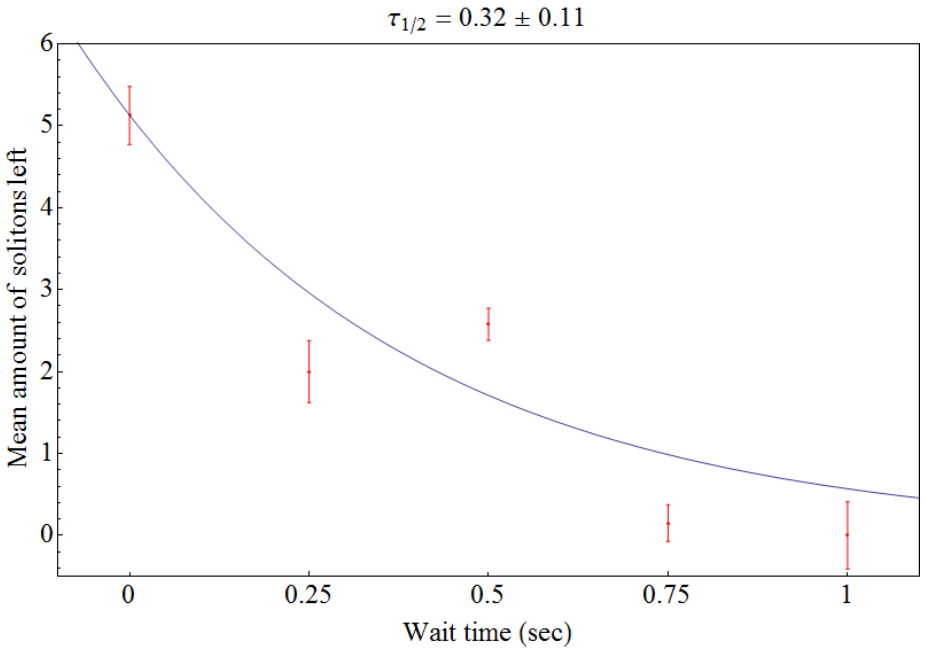

(a) Axial condensate size = 400 px

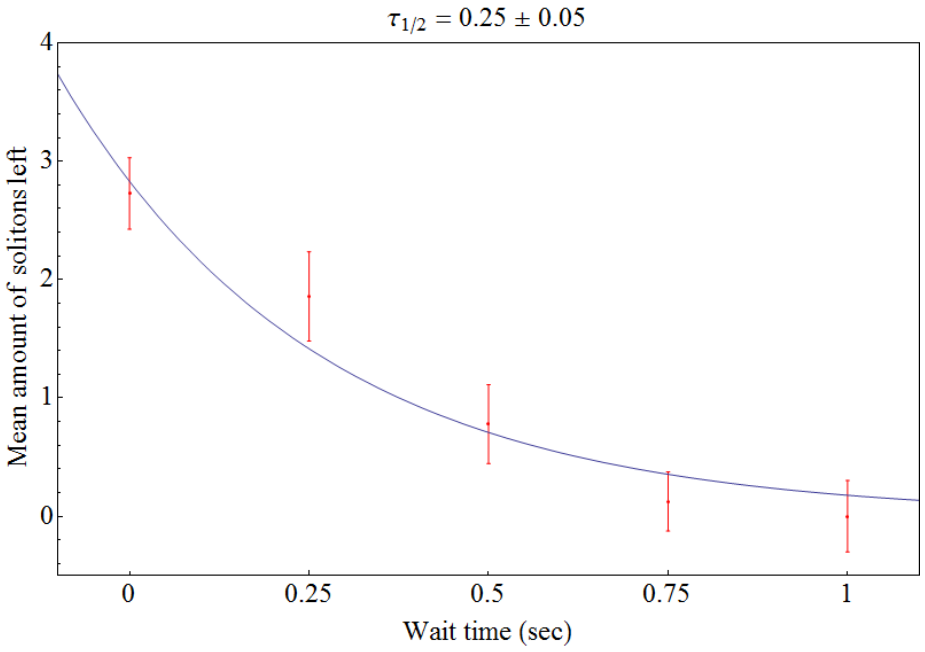

(b) Axial condensate size = 450 px

Figure 6: Analysis of the half-life time for two different condensate sizes. Aspect ratio = 55. Quench time = 2 sec.

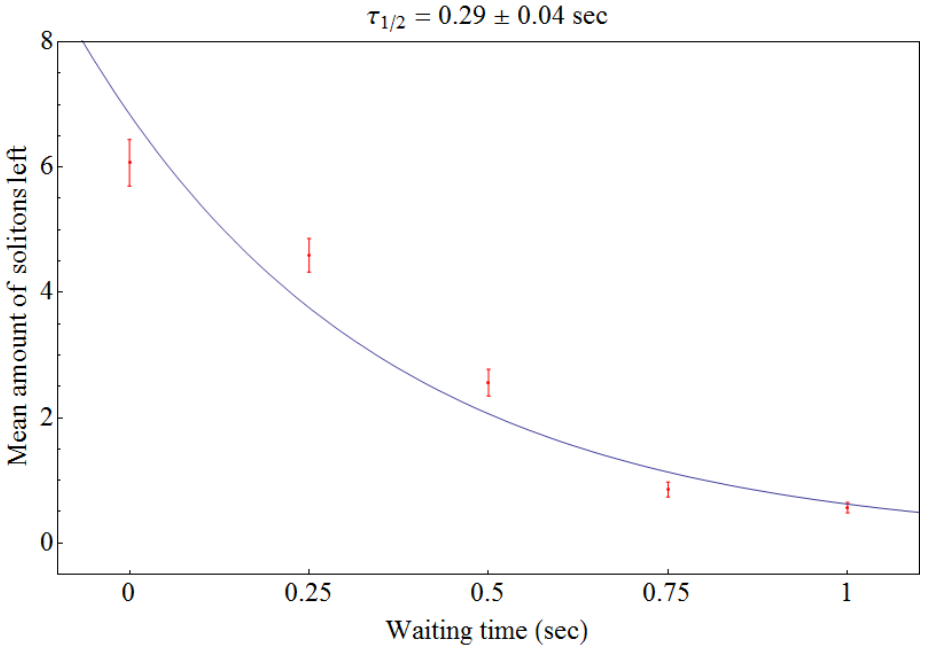

Figure 7: Measurements of the exponent in the aspect ratio 55 configuration.

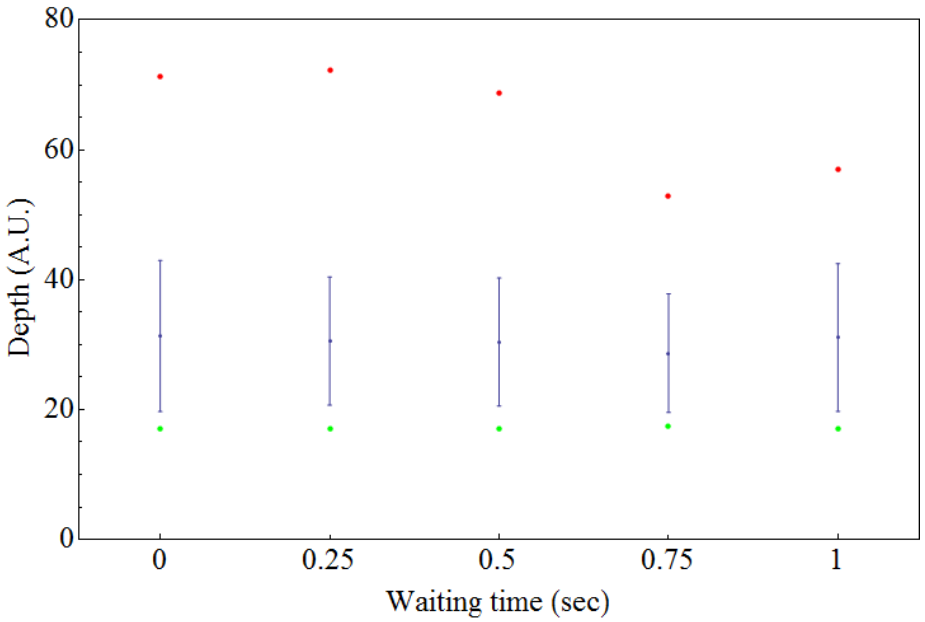

Figure 8: Plot of the heights of the peaks found through the analysis routine. In blue, the means along with their standard deviations are given. The red points are the maxima and the green points are the minima.

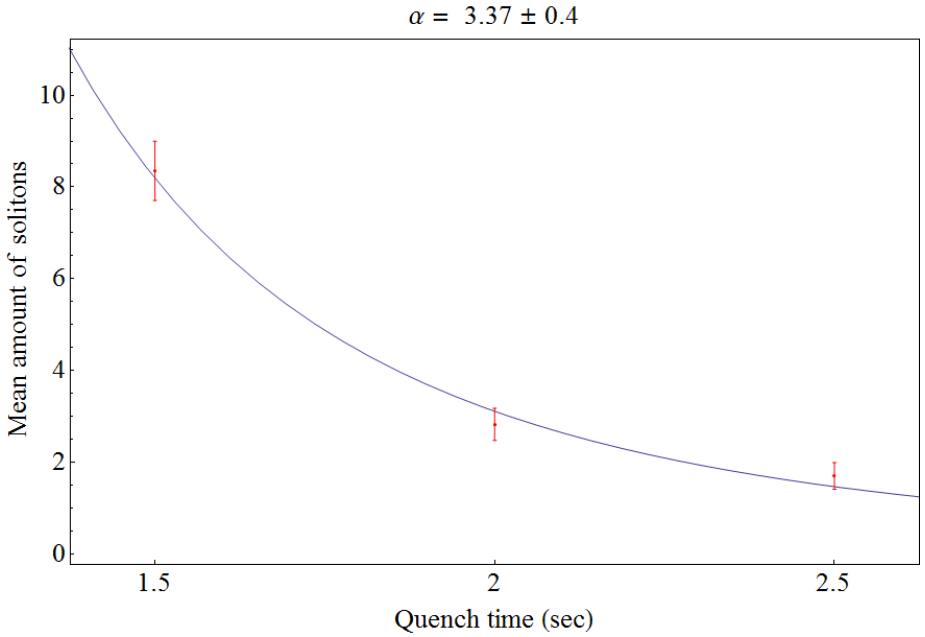

Figure 9: Early measurements of the exponent in the aspect ratio 55 configuration. Data points are given in red, while the fitted curve is blue.

4.4 Exponent

With the data on decay times in mind, we attempted to determine the exponent through means of the predictions done by the KZM.

Preliminary measurements were done to determine the exponent as well and were in fact the earliest measurements done during the research. The result of these measurements are shown in Figure 9, and indicate that the exponent is in the order of 3.4. These early measurements were not designed to accurately determine the exponent, but rather as a proof of concept. The measurements were strongly in agreement with the exponential model given by the KZM. In order to attempt to determine the exponent more accurately, a larger sample size is needed. This was done by aiming for around 50 measurements per quench time, which should then at least leave 20 images that satisfy the size requirement. The results of this series of measurements is shown in figure 10. What immediately stands out is that this result is not very well in agreement with the preliminary measurements, although it is within the standard deviation, and that the fitted curve does not neatly go through the data points. In fact, the second data point is higher than the first one, suggesting that the amount of solitons grows with the quench time, which goes firmly against the KZM. The same goes for the third and fourth data points, although the difference here is less pronounced. We find an exponent of 6.00 ± 1.83.

Since the quench times are in the order of seconds, while the decay time is in the order of 0.3 seconds, the decay of solitons is a significant factor. One way of attempting to correct for this is by multiplying each data point by $2^{\frac{\tau_Q}{\tau_{1/2}}}$,

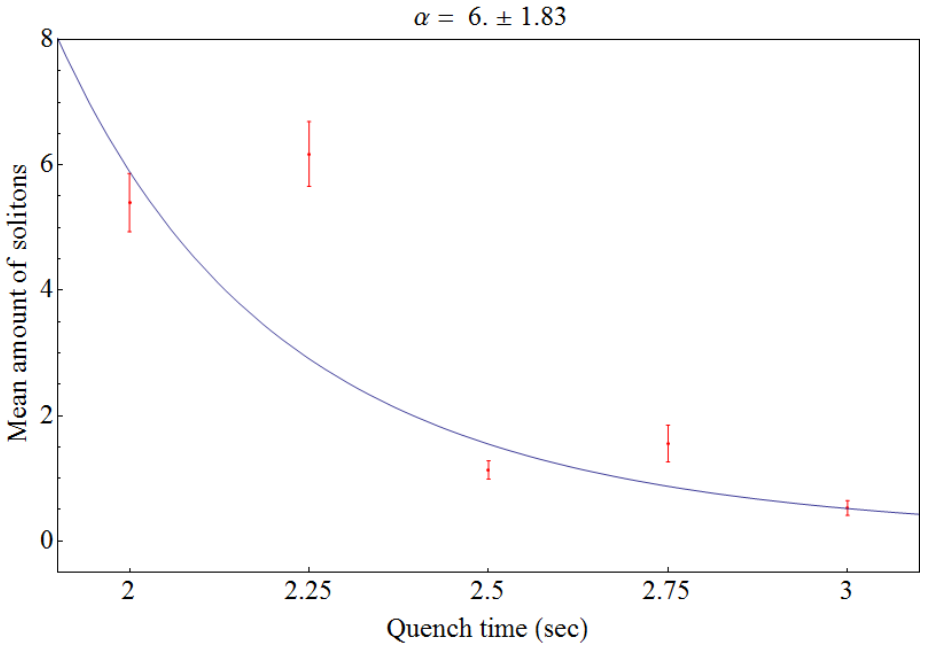

Figure 10: Measurements of the exponent in the aspect ratio 55 configuration. Data points are given in red, while the fitted curve is blue.

which would compensate for the decay. The results of this correction for values of the half-life time as found in the previous section are given in Table 1. Note that a value for the half-life time of ∞ corresponds to no correction at all. It is immediately clear that a slight difference in the half-life time has a large influence on the exponent that is found.

However, the method of correction described above is very naive and does make the assumption that all solitons are formed exactly at the start of the quench and that the decay is actually exponential. The first is not true, since the start of the quench is selected to be above the critical temperature and the sample is inhomogeneous, which implies that there is no certain time at which all of the solitons form. The second assumption has already been treated in Section 4.2. To compensate for the first assumption, another factor, f, could

$\tau_{1/2}(s)$	α	σ_α
∞	6.00	1.83
0.33	0.84	1.79
0.31	0.47	1.79
0.29	0.05	1.8
0.27	-0.45	1.82
0.25	-1.04	1.83

Table 1: The effect of variation in the half-life time on the determined value for α.

be introduced, which is a value between 0 and 1 that indicates where in the quench the critical temperature is crossed, 1 being at the start and 0 being not at all The correction factor then becomes $2^{f*\frac{\tau_Q}{\tau_{1/2}}}$. This would compensate for the fact that the solitons are not formed immediately at the start of the quench, but since we do not know exactly when they are formed in the quench, it is just merely guessing and that will not further help our understanding of the process.

Based upon the above, an interval can be given in which the exponent α may reside. First of all, the exponent has to be strictly positive. Negative values would indicate an increase of the amount of solitons one finds as the quench is slowed, which is clearly not the case. If the exponent were to be zero, the amount of solitons would not depend on the quench time at all, which goes against the results found during this research and others. So we expect the value for α to be larger than 0, so we shall estimate the lower boundary to be around 0.5. An upper bound is harder to impose and has to come from the fact that the critical exponents have to be positive. Since the exponent is universal and the values found in lower aspect ratios indicate that the value of the exponent is around 2 without correcting for the lifetimes, we estimate an upper bound of 2. So given the physical arguments and the results we obtained, a value between 0.5 and 2 seems most likely. Mean-field theory predicts the value $\alpha = 1$, while in Ref. [4], the value $\alpha = \frac{7}{6}$ is predicted. While our values are not conflicting with these predictions, the uncertainty is too large to draw conclusions on which value is the correct one.

4.5 Influences and miscellaneous measurements

As with all experimental researches, you want to know as many factors that could possibly influence your final result as possible. As stated in Ref. [6], the amount of particles in the condensate, and with that the density of the condensate, is of influence. When the density is lower, more solitons are formed for a given quench time than if the density were to be higher. It is clear when looking at the results on the decay time between two different size as given in Figure 6 that for the same quench time and waiting times, there is a clear difference in the amount of solitons that are found. As can be seen, the density is indeed a factor, so therefore in the analysis it is paramount that only condensates of roughly the same size are compared.

We also investigated the influence of aspect ratio on the exponent. This is interesting, because different decay mechanism and instabilities may become important at different aspect ratios. While the critical exponents are supposed to be universal, they are still dependent on the dimensionality of the system. The majority of the measurements in this research were done at an aspect ratio of around 55, which is sometimes referred to as quasi-1D. In this series we studied a few different aspect ratios lower than 55, being 25, 10 and 6. In Appendix B, images from these measurements are shown. As it appears, it is more difficult to produce solitons in lower aspect ratios, as we need to decrease the quench time to below a second in order to produce more than 5 solitons in the case of aspect ratio 10, while that same quench time would elicit chaos in the aspect ratio 55 configuration. As can be seen in the images, extracting the amount of solitons is very difficult and only a rough estimate can be given for

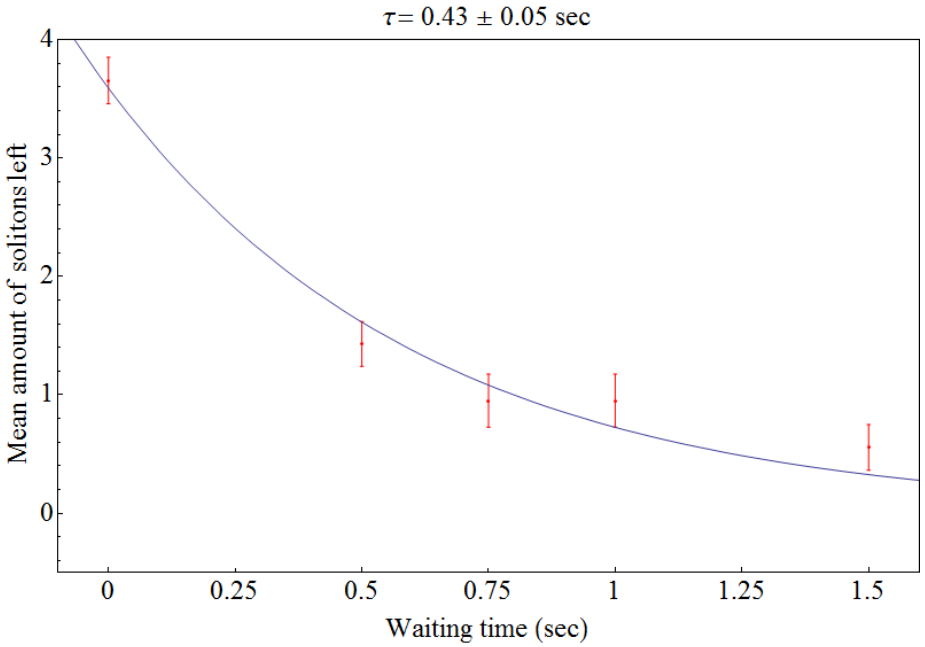

Figure 11: Measurements of the decay time in the aspect ratio 15 configuration. Quench time = 2 sec

the exponent. This was done by manually checking images from the series and for each quench time select six to eight measurements, from which an estimation of the mean amount of solitons was made, which were then used in the regular fitting procedure. From this we find that for an aspect ratio of 25 the value for α is around 2 and for aspect ratio 10 this value is around 2 as well. For aspect ratio 6 it was too difficult to count the solitons to give even a rough estimate of the value for α.

The decay time was also determined for an aspect ratio of 15. Figure 11 shows the results of these measurements. Interestingly enough, the value for $\tau_{1/2}$ actually seems to be larger for this aspect ratio than it is for aspect ratio 55, while, based on the theory, one expects that the lifetime is longer for the higher aspect ratio. The reason for this is unclear and requires more research.

A noteworthy finding is that for the measurements done on aspect ratio 6, even though a value for α could not be estimated, solitons as well as vortices are present, which means that the transition between the regime of solitons and the regime of vortices is not a discrete step, but rather a continuous transition. Figure 25 Shows a neat example of a vortex. As shown, the exponent seems smaller for the smaller aspect ratios. We have not investigated why this happens, but the longer lifetime in the lower aspect ratios may be of influence on this. This may be related to the fact that a quicker quench is needed to produce solitons in lower aspect ratios, which means less time to decay is given, giving us an exponent that is closer to the real value of the exponent. The measurements on these aspect ratios were done before it became clear that the decay time was a significant factor and we have not fully investigated the influence of the

AR	α	σ_α	$\tau_{1/2}(s)$	$\sigma_\tau(s)$
55	6.00	1.83	0.29	0.04
25	1.9	0.2	-	-
15	-	-	0.43	0.05
10	2.15	0.20	-	-
6	-	-	-	-

Table 2: Overview of the values that were found per aspect ratio.

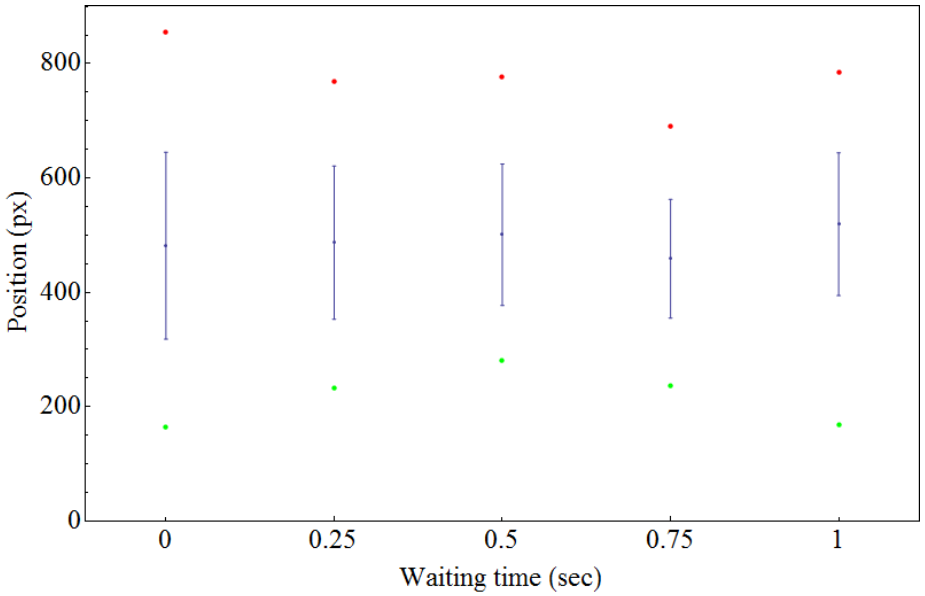

Figure 12: Plot of the positions of the solitons found through the analysis routine. In blue, the means along with their standard deviations are given. The red points are the maxima and the green points are the minima.

aspect ratio on the decay time. This was also done before it became clear that the condensate size was a relevant factor as well, so we did not take that into account either during the measurements. The lower the aspect ratio gets, the harder it is to properly distinguish solitons, which is one of the reasons why we ultimately decided to do the majority of our measurements in the highest aspect ratio.

An overview of the values that were found for the exponent and the lifetime per aspect ratio is given in Table 2. Note that the most recent results per aspect ratio are displayed, leaving out the preliminary measurements.

Another prediction of the KZM is that the solitons will only form near the center of the trap [4]. We attempted to test this prediction by also recording the positions of the solitons in the condensate during the analysis to see if there were any preferential positions. Note that solitons are not stationary, so merely recording the positions of one measurement is insignificant on its own. These measurements are shown in Figure 12. The means of the positions indeed seem

to be situated in the middle of the image, corresponding to the middle of the condensate. The minima and maxima of the soliton positions fluctuate, but do not show a clear pattern. From this we conclude that the solitons are spread out through the condensate, but we cannot conclude that the solitons are formed in the center only, since the solitons are not stationary and have had time to move during the last part of the quench step. Once again, PCI could possibly provide a method of probing the early stages of the formation of the condensate, which could provide valuable data.

5 Conclusion

Solitons were formed by shock cooling the last stage of evaporative cooling, forcing the temperature below the critical temperature swiftly throughout the trap, as described by the Kibble-Zurek mechanism. We varied the quench time in order to test the prediction done by the KZM that the amount of solitons that form obey a power law in the quench time, with an exponent α. Initial results were promising as it seemed that the amount of solitons did indeed obey a power law in the quench time. The main goal was to determine the value of α, which is composed of the critical exponents of the transistion.

Since solitons can decay, we investigated the timescale on which the decay happens by defining a half-life time. This half-life was determined experimentally by fixing a quench time and introducing a waiting time before the time of flight and imaging. This way the solitons were given time to decay before being imaged. This half-life time turned out to be in the order of 0.3 seconds, which has a profound impact on the value for α, since the quench times that were considered for the majority of the measurements were in the order of several seconds. The lifetime was quantified as a half-life time An attempt was made to correct for this decay by applying a correction factor to each data point. The lifetime turned out to be so short in comparison to the studied quench times that a small deviation in the lifetime made a big difference in the value that was found for α. Instead of being able to accurately determine a value for α, we determined that the value for α most likely resides between the values of 0.5 and 2, based on both physical arguments and measured data. This is in agreement with predictions for α in the order of 1, as given by mean-field theory and Ref. [4].

As stated in Ref. [6], the amount of solitons by a given quench time dependents on the density. We have done measurements on this as well and were able to confirm that the mean amount of solitons that one finds at a given quench time is larger for smaller condensates than the mean amount found in larger condensates. As a result, the size of the condensate was made a criterium during the analysis of the measurements in order to only compare condensates of roughly the same size.

The effect of different aspect ratios was also investigated. Since α is composed of the critical exponents, it is expected to be universal, however it is still dependent on the dimensionality of the system. THe majority of our measurements were done on condensates of aspect ratio 55, which is sometimes considered to be quasi-1D. Measurements on condensates of lower aspect ratio turned out to be more difficult to analyze, but still estimates for the value of α, without correcting for decay times, were made and indicate that the value α becomes lower with aspect ratio. This is possibly due to the shorter quench times needed to produce solitons, allowing for less decay and a more accurate determination of α without having to correct for the decay time. For an aspect ratio of 6 we find that solitons as well as vortices are produced.

6 Discussion

As with most experimental studies, one won't obtain perfect data and one won't fully understand every quirk that happens during the course of the research. Should you know all these details beforehand, there would be no need to do any of this research after all. This experiment was, once again, no exception to this and I would like to devote this section to those points of uncertainty that could have skewed the numbers and introduced uncertainties in the final results.

First of these points is the decay of solitons. As seen in previous sections, at finite temperatures at least, solitons are not stable and will eventually lose their energy and dissipate. Several methods of dissipation have been described in the section on soliton decay, but theory alone doesn't tell us which of these mechanism is the most prevalent in our experiment. We have done some preliminary research on this as shown in the results section, but that hasn't given us any conclusive evidence on which of the mechanism is the most prevalent in our experiment.

Another phenomenon is the occurrence of notches in the density from one of the sides, which we have dubbed "half-solitons". These half-solitons resemble solitons in that they are a density depletion, but they don't seem to go all the way through the condensate, only making it partly through the condensate before they stop making a density depletion. An example of one such half-soliton is shown in Figure 14. I have been unable to find an explanation for this particular phenomena, especially given the nature of the formation of these solitons. The only explanation I can come up with is that these are vortices that are leaving the condensate after being formed through the snake instability, but this is merely a wild guess on my part and in no way supported by any evidence.

A last point that is more human error than the previous points is the counting of the solitons. In this research a program written be me was used to automatically count solitons. This program seems to work fine, but has its limitations in its accuracy. It starts to become problematic when the quench times are low and thus the amount of solitons present will be high. These solitons are capable of overlapping each other and start to lay very close to one another, which can make it very difficult for the program to separate them, thus counting less solitons than are actually present. Half-solitons may also form a problem, because when they don't deplete the condensate very far, they may give a peak in the spectrum that is not high enough to be above the counting threshold. Since these half-solitons are clearly defects, they should be counted.

7 Outlook

As with any research, with this one being no exception, some questions have been left unanswered and other questions have emerged during the course of this project. Seldom do all questions get answered and more often than not does one research project pave the way for another. Most of the questions that have arise during the course of this research has already been mentioned in the relevant sections where they first arose, but they will be summarized here for convenience.

First and foremost, the question that I initially set out to answer, what the values of the critical exponents are, is still left unanswered. The lifetime of the solitons is too short in comparison with the quench times that we have used, which manifested itself in the large uncertainty in the determination of the exponent α. One way to improve this would be to create a system in which the mean lifetime of the solitons is in the order of seconds instead of a third of a second.

Another question is that of the decay mechanism. As described in section 2.4.4, most of the decay mechanisms described are expected to be suppressed. Still the decay time is found to be in the order of a third of a second. So we do not fully understand the system as of yet. A way to gain understanding of the mechanisms at work would be to utilise non-destructive imaging in order to be able to track solitons through their lifetime. This way, if the snake instability is a dominant mechanism, this should be well visible as the breaking up into vortices will be made visible. The the two other mechanisms will be more difficult to distinguish from one another, as both will cause the soliton to gradually lose energy. To accomplish this, there is another problem that will need to be solved first, which is the resolution of the imaging. The above will need to be done in situ, where the width of solitons is in the order of the healing length, which is smaller than a micron. So either the resolution of the imaging needs to be improved, or a system needs to be devised in which the healing length is greater than 10 micrometer. As seen in eqn. 20, this can be done by either increasing the scattering length or lowering the density. The latter is more easily done than the former.

Another feature that could possibly be implemented in the experiment would be the ability to levitate a condensate, by compensating for the gravity, after the magnetic trap is turned off for the time of flight. This will not only allow for longer expansion times, since the ToF is no longer limited to the time it takes for the condensate to fall to the bottom of the chamber, but it will also be very convenient for the switch between PCI and AI. Normally, the trap is turned off and the condensate expands while falling due to gravity. To image this, the lens will have to be moved in order to get the condensate in focus after the ToF. For PCI, this is done in situ, so the lens will have to be moved back in order to shift the focal point once more. If this feature is implemented, both for PCI and AI the lens can remain in the same position, allowing for faster switch times. As seen in the images in section **??**, for the lower aspect ratios the condensate is optically still reasonable dense. Longer expansion times can benefit the measurements done on these aspect ratios.

8 Appendix A: Summary in laymen's terms

This section is meant for those who would like to know what I have researched in the past year, yet have no background in physics. I shall attempt to explain the main points of my thesis whilst omitting the technical details and terms.

One of the fundamental properties of atoms is that their energy is not continuous, but rather a discrete amount, dictated by quantum mechanics. Their energy also cannot be equal to zero, there is a minimum energy that an atom must have. Atoms also have a quantum mechanical property called spin, which is somewhat like the earth spinning around its own axis, but in reality no classical analogy can truly be made. This spin has a number attached to it, which is either an integer amount, so $0, 1, 2 \cdots$, or half-integer, such as $\frac{1}{2}, \frac{3}{2}$ etc. Particles with an integer amount of spin are called bosons and those with half-integer spin are called fermions. A crucial difference between the two is that bosons are allowed to be in the exact same energetic state, while fermions are not. This is due to another quantum mechanical principle. When a lot of bosons together get into the lowest energetic state, known as the ground state, they form a new state of matter known as a Bose-Einstein condensate (BEC).

In order to achieve this, we need to cool down the atoms to almost absolute zero, 0 Kelvin or -273.15 degrees Celcius. This is not an easy task, of course, and in order to achieve this we use lasers and magnetic fields. The use of lasers might feel counterintuitive, so I shall explain the principle of laser cooling using the usual analogy. You can compare it to throwing tennis balls at a truck coming at you. The tennis ball will hit the truck, absorb a bit of its momentum and fly off because it got knocked away. So now the truck has been slowed down a very tiny amount. Throwing more and more tennis balls will slow the truck down further and further and eventually the truck will be stopped. In this analogy the truck is the atom that needs to be slowed and the tennis balls represent the light particles, named photons, from the laser beam. This may seem like a very inefficient way of cooling, but now consider that the laser shoots about ten million photons a second and is capable of slowing down an atom going 800 m/s down to 30 m/s in a matter of milliseconds. This is sufficient to cool down an atom of around 300 degrees Celcius to around 1 K(elvin) or -272.15 degrees Celcius. Pretty cold? Yes, but in order to achieve condensation it needs to be cooled down even further until it's around 10^{-6} K. To do this, we use the properties of the atoms to trap them in a magnetic field. Particles in this trap will now mingle a bit and every now and then collide with another particle, thus giving one particle a higher energy and the other a lower one. If we now make a hole in the upper part of the trap where only higher than average energy particles can reach, those particles can escape the trap and the average energy of the remaining particles is lowered a bit, which also means that the average temperature is lowered a bit. Repeating this process and slowly lowering the height of the hole in the trap will eventually allow us to cool the atoms down far enough for the condensed state to be reached. We have now made ourselves a Bose-Einstein condensate.

Now why would we want go through this complicated process anyway? Condensates like this one show interesting properties and exhibit quantum mechanical features on a much larger scale than one would normally find, which makes re-

searching them a lot easier than it would be otherwise. What I have done is take that last cooling step and do it much more quickly than you would normally do. When done quick enough, interesting things happen to the condensate when it is being formed. When cooled quick enough, not just one condensate forms, but multiple different ones can form. When those grow further and eventually meet, they need something to bridge the difference between the condensates. This something is called a soliton and can be observed as a stripe of lower density through the condensate. What I've been studying is how many of these solitons form as a function of the speed at which the cooling step is performed. This will let me find a certain number, called the critical exponent, that will allow me to say something about the type of transition the transition into the condensed state is.

Besides that I also studied the lifetime of those solitons. Solitons do not live forever and gradually lose their energy and depth and eventually disappear. I looked at the timescale on which they disappear, because that might be an important factor when counting the amount after a longer cooling time. As it turns out, it takes about a quarter of a second for about half to disappear. Since I am looking at cooling times in the order of seconds, this is a very important factor and another complication for me to consider.

As it turns out, the lifetime of solitons is pretty short, half of the solitons will have disappeared after about a third of a second, while the speed of the last bit of cooling is a few seconds, making this an important factor. So as it turns out, determining the critical exponent is a lot harder than I had hoped, because I need to correct for the lifetime. As it turns out, a very little change in the lifetime will cause a large difference in the value I find for the critical exponent, so I can't say for certain what the number actually is.

So in the smallest nutshell that I can possibly find: I spent a year counting stripes to determine a couple of numbers, which turned out to be pretty difficult.

9 Appendix B: Images of measurements

To avoid filling up the results section with images and to give a better idea of what our measurements look like, a few images of the different aspect ratios we have done measurements on will be presented here. Among these images are a few interesting results displaying effects such as vortices and half-solitons.

9.1 Aspect ratio 55

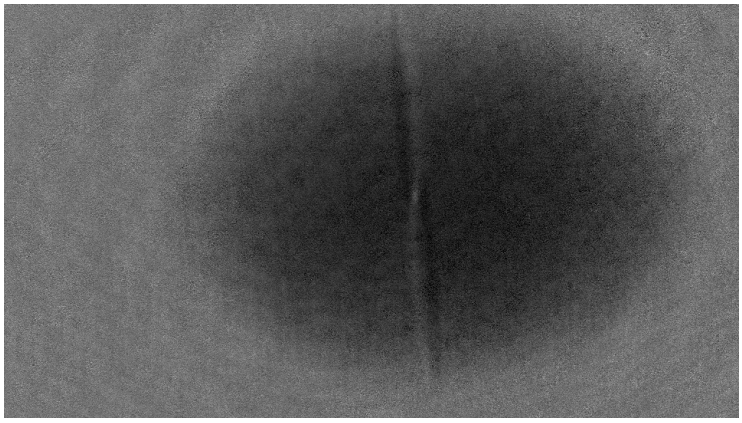

Figure 13: Quench time = 2 sec, waiting time = 0.75 sec. Note that the soliton does not appear to be a straight line.

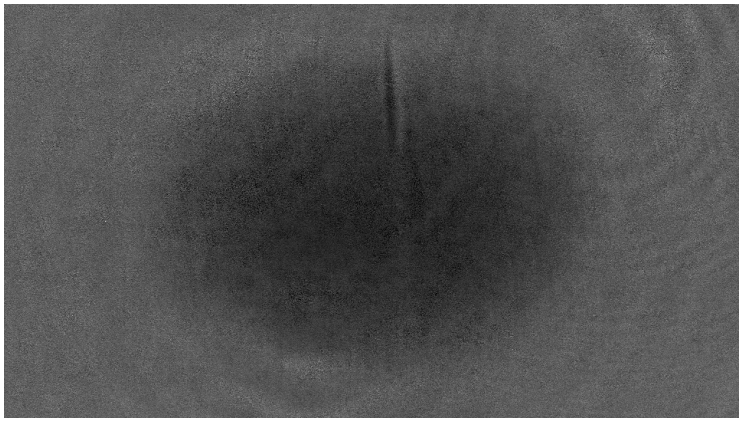

Figure 14: Quench time = 3 sec. Note the half-soliton

9.2 Aspect ratio 25

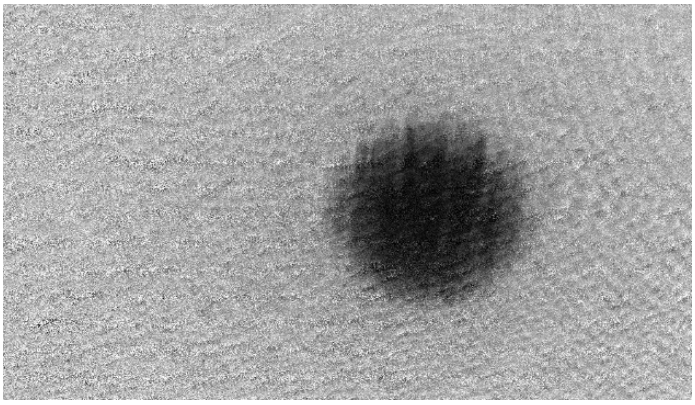

Figure 15: Quench time = 1 sec.

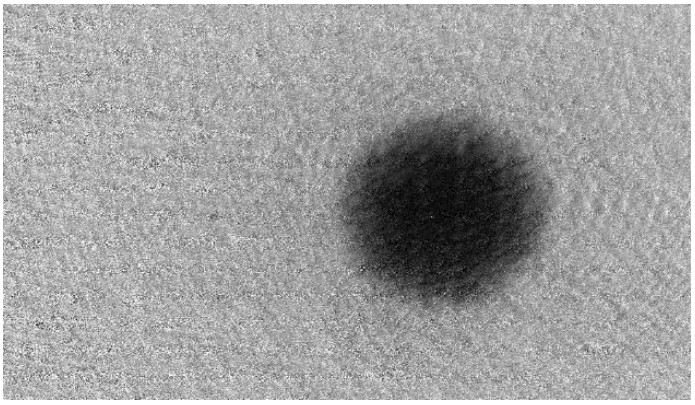

Figure 16: Quench time = 1.4 sec

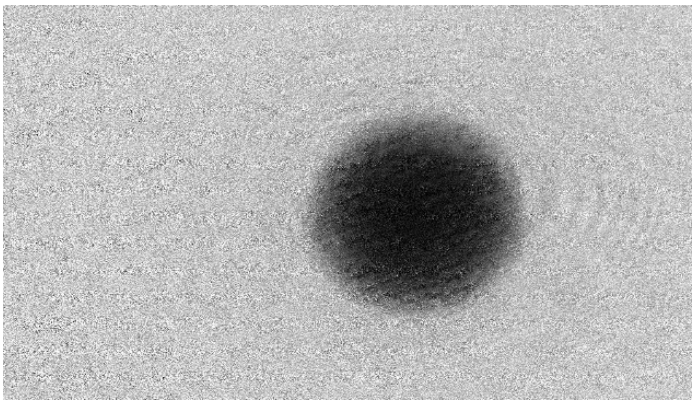

Figure 17: Quench time = 2 sec.

9.3 Aspect ratio 15

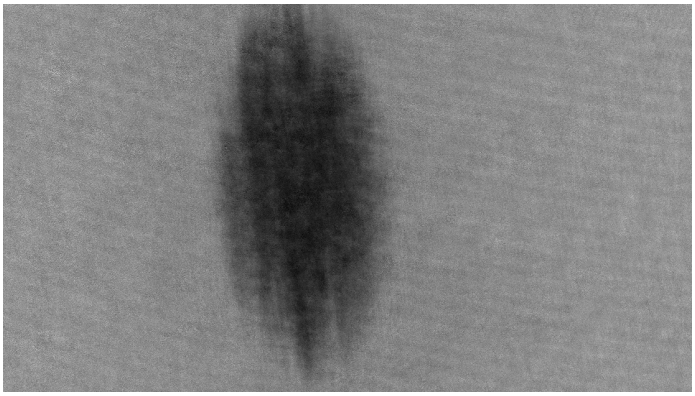

Figure 18: Quench time = 0.8 sec, no waiting time

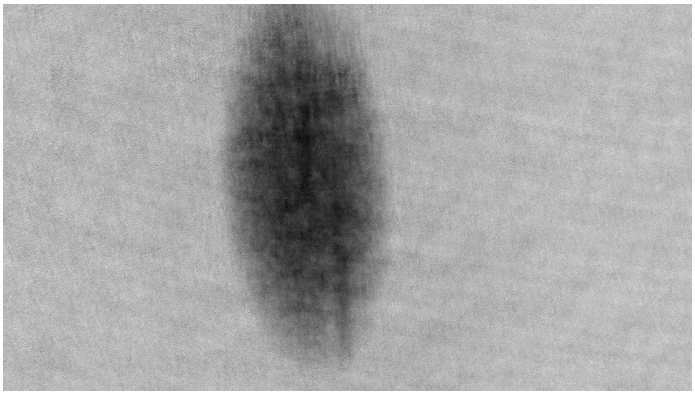

Figure 19: Quench time = 0.8 sec, waiting time = 0.75 sec

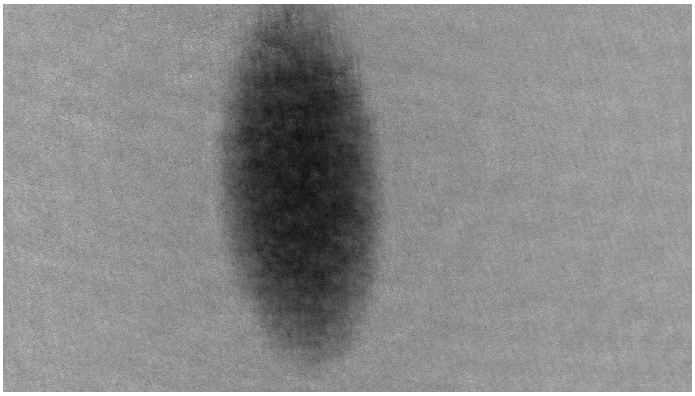

Figure 20: Quench time = 0.8 sec, waiting time = 1.5 sec

9.4 Aspect ratio 10

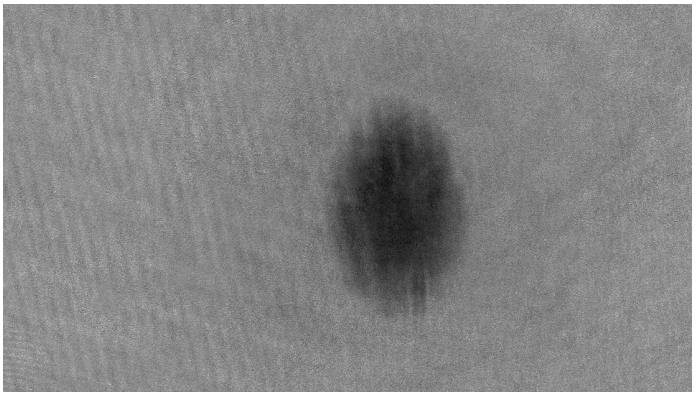

Figure 21: Quench time= 0.8 sec

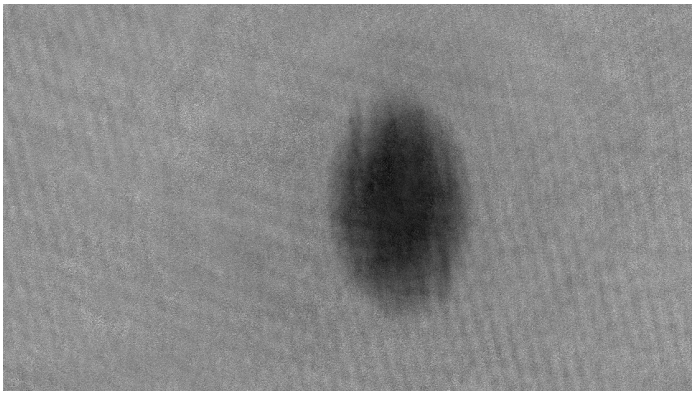

Figure 22: Quench time= 1.2 sec

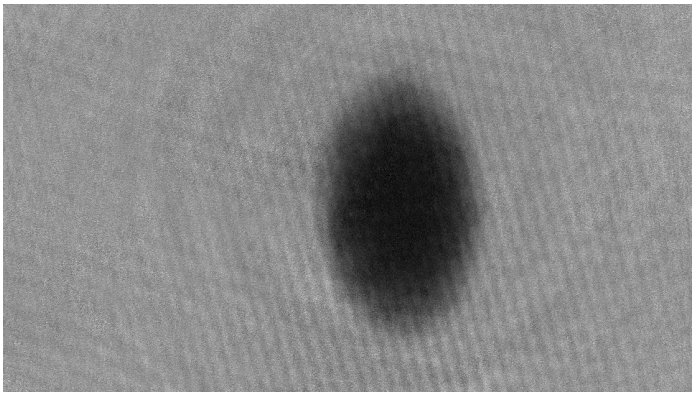

Figure 23: Quench time= 2 sec

9.5 Aspect ratio 6

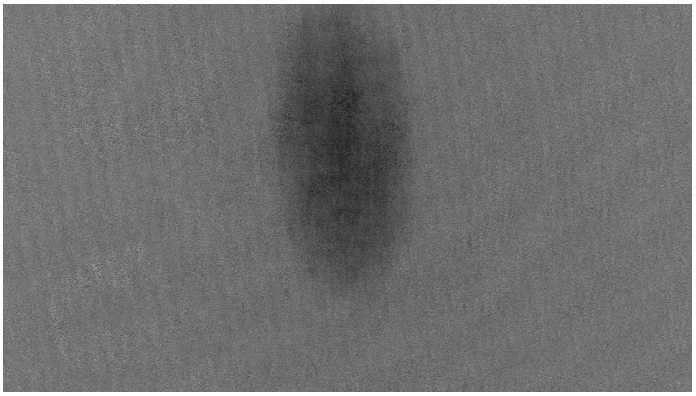

Figure 24: Quench time= 0.6 sec

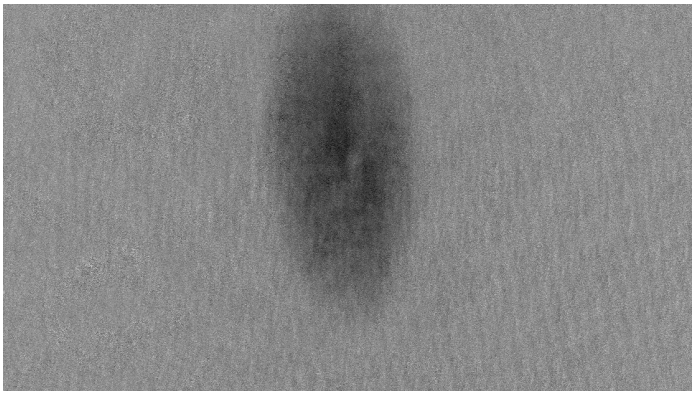

Figure 25: Quench time= 1 sec. Note the vortex in the middle.

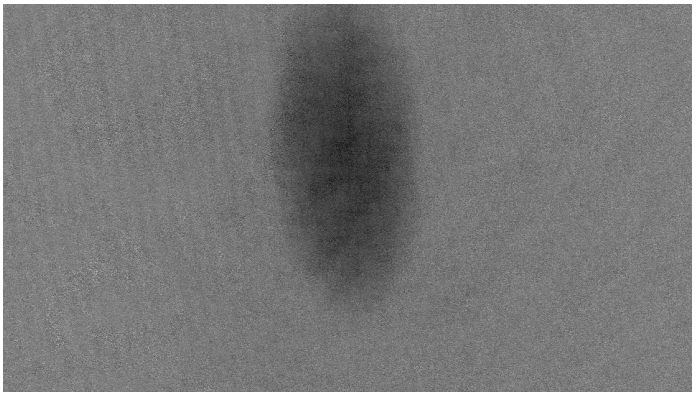

Figure 26: Quench time= 1.2 sec

Acknowledgements

It is only appropriate that I extend my gratitude to the people that have been integral to the completion of this thesis. The first of these is my daily supervisor, Pieter Bons, PhD student in our group, for helping me with doing the experiments I wanted to do and helping me to make sense of it all and explaining to me the things I wanted to know about the experiment. I would also like to thank prof. Peter van der Straten for allowing me to run around the lab for about a year and giving me the opportunity to challenge myself ever further. I am also grateful for the rest of the BEC group, my fellow students, that were always challenging my every move and providing useful input that allowed me to make sure that I knew what I was doing.

The technical staff of the nanophotonics group, ing. P. Jurrius, ing. C. de Kok, ing. F. Ditewig and dr. D. Killian, also deserve my thanks for keeping the experiment running throughout the year.

Finally, all of my friends and family that have supported me throughout the year have my deepest thanks. Especially in the last few weeks up to the deadline, those of you who convinced me to not spend every waking moment working and invited me out to have some downtime have been paramount to the successful completion of this research.

References

[1] C. Pethick & H. Smith. *Bose-Einstein condensation in dilute gases*. Cambridge University Press, 2002.

[2] T. W. B. Kibble. Topology of cosmic domains and strings. J. Phys. A: Math. Ge., Vol. 9, No. 8 (1976)

[3] R. Meppeling. *Hydrodynamic Excitations in a Bose-Einstein condensate* (2009).

[4] W. H. Zurek. Causality in Condensates: Gray Solitons as Relics of BEC Formation. *Phys. Rev. Lett.* **102**, 105702 (2009)

[5] A. del Campo, T. W. B. Kibble, W. H. Zurek. Causality and non-equilibrium second-order phase transitions in inhomogeneous systems. arXiv:1302.3648v2 (2013)

[6] G. Lamporesi, S. Donadello, S. Serafini, F. Dalfovo, G. Ferrari. Spontaneous creation of Kibble-Zurek solitons in a Bose-Einstein condensate. *Nature Physics* 2734:656-660 (2013)

[7] Th. Bush & J. R. Anglin. Motion of dark solitons in trapped Bose-Einstein condensates. arXiv:cond-mat/0001360v1 (2000)

[8] A. E. Muryshev, G. V. Shlyapnikov, W. Ertmer, K. Sengstock, M. Lewenstein. Dynamics of dark solitons in elongated Bose-Einstein condensates. arXiv:cond-mat/0111506v1 (2001)

[9] N. G. Parker, N. P. Proukasis, C. S. Adams. Dark soliton decay due to trap anharmonicity in atomic Bose-Einstein condensates. arXiv:0906.4877v1 (2009)

[10] J. Smits. Formation of Faraday patterns in cigar-shaped Bose-Einstein condensates (2013).

[11] M. van 't Woud, J. van der Tol. *Particle flux: Slow and fast* (2012).